1622

178
1/23/80

DR. 564

DECEMBER 1979

PPPL-1622
UC-20g

MASTER

BALLOONING-MODE THEORY OF TRAPPED-ELECTRON INSTABILITIES IN TOKAMAKS

BY

C. Z. CHENG AND L. CHEN

PLASMA PHYSICS LABORATORY

PRINCETON UNIVERSITY
PRINCETON, NEW JERSEY

This work was supported by the U. S. Department of Energy Contract No. EY-76-C-02-3073. Reproduction, translation, publication, use and disposal, in whole or in part, by or for the United States Government is permitted.

Ballooning-Mode Theory of Trapped-Electron Instabilities in Tokamaks

C. Z. Cheng and Liu Chen

Plasma Physics Laboratory, Princeton University,
Princeton, NJ 08544

Employing the ballooning-mode formalism, the two-dimensional eigenmode equation for trapped-electron instabilities in tokamaks is reduced to a one-dimensional integro-differential equation along the magnetic field lines; which is then analyzed both analytically and numerically. Dominant toroidal coupling effects are due to ion magnetic drifts which create quasi-bounded states. The trapped-electron response can be treated as perturbation and is found to destablize the quasi-bounded states.

In tokamaks, the trapped-electron instability is basically a drift wave driven unstable by the presence of trapped electrons.[1] It has been suggested that the trapped-electron instability may give rise to anomalous transports in high temperature tokamaks. A complete understanding of the linear eigenmode problem, however, is essential for studying its nonlinear behavior and consequences. Since dynamics associated with ion magnetic drifts and trapped electron terms can lead to coupling between different poloidal harmonics, the linear eigenmode analysis of the trapped-electron instabilities is intrinsically two-dimensional. Recent numerical calculations[2] of the trapped-electron instabilities by employing the ballooning-mode formalism[3] have yielded good agreements with a two-dimensional code[4] embodying identical physical assumptions. It is the purpose of the present work to study the two-dimensional trapped-electron instabilities analytically by using the ballooning mode formalism.

The damping effect of drift waves in a sheared magnetic field is related to the anti-well potential in which wave energy convects away from the mode rational surface.[5] However, in a toroidal plasma the curvature and magnitude of the magnetic field is not uniform over a magnetic surface. This nonuniformity of the toroidal field can cause coupling between the eigenmodes which centered on different mode rational surfaces.[6] Recently, we have studied the two-dimensional drift wave eigenmodes in a toroidal plasma[7,8,9] using the ballooning mode formalism. Due to toroidal coupling effects of ion magnetic drifts, two types of eigenmodes are identified: (1) The slab-like (Pearlstein-Berk type) branch, which has anti-well potential structures, is found to experience enhanced shear damping due to the toroidal coupling. (2) The toroidicity-induced eigenmode branch, which has no counter part in slab geometry, is characterized by potential structures with local potential wells which inhibit convection of wave energy. In the absence of electron dissipation, it corresponds to a quasi-marginally stable, quasi-bounded state and experience negligible shear damping through tunneling leakages. With the inclusion of electron Landau damping or electron-ion collision, it becomes absolutely unstable. The existence of the toroidicity-induced eigenmodes clearly indicates that, contrary to conventional thinking, toroidal coupling effects due to ion magnetic drifts cannot be simply regarded as perturbations to the slab eigenmode branch. In this respect, one may think that the toroidal coupling effects associated with the trapped electron may also play the role of introducing new eignemode branches in addition to the usual destablizing role. However, as we will show later, the trapped-electron toroidal coupling effects come in through trapped electron average of the fluctuation potential and only serve to enhance the toroidal coupling effects due to ion magnetic drifts.

Previous analytical studies[10,11] of the two-dimensional trapped electron instability were focused on the slab eigenmode branch with ion magnetic drifts neglected and trapped-electron contributions considered as perturbations. In this work, we have found that the most unstable trapped electron mode is related to the toroidicity-induced eigenmode branch induced by the toroidal coupling effects due to ion magnetic drifts.

Employing the ballooning-mode formalism, the two-dimensional eigenmode equation for trapped-electron instability is reduced, in the lowest order, to a one-dimensional integro-differential equation along the magnetic field lines. The radial structure can be determined by a WkB procedure in the next order which provides small corrections to the eigenfrequency.[2] The analytical solutions of the 1D integro-differential equations are presented for the toroidicity-induced eigenmode branches. The analytical solutions are then compared with the numerical solutions of the 1D integro-differential equation performed by using the cubic B-spline finite element method[12] in order to provide more understanding.

We consider long wavelength ($k_\perp \rho_i \ll 1$) electrostatic drift waves in a large aspect ratio, axisymmetric tokamak with concentric, circular magnetic surfaces. The perturbation Φ can be written in the form

$$\Phi(r,\theta,\zeta,t) = \sum_j \Phi_j(s)\exp[i(m_o\theta+j\theta-n\zeta-\omega t)] \tag{1}$$

where (r,θ,ζ) correspond to the minor radial, poloidal and toroidal directions respectively, $s = (r-r_o)/\Delta r_s$, r_o is the minor radius of the reference mode rational surface with $m_o = nq(r_o)$, $\Delta r_s = 1/k_\theta \hat{s}$, $k_\theta = m_o/r_o$, $\hat{s} = (rq'/q)_{r=r_o}$ and $|j| \ll |m_o|$. The tokamak magnetic field is given by $\underline{B} = B_o(1-\varepsilon\cos\theta)(\hat{\zeta}+\varepsilon/q\ \hat{\theta})$.

The two-dimensional eigenmode equation for the trapped-electron mode in the limit $(\omega_{b,t})_i < \omega < (\omega_{b,t})_e$ is given by[1]

$$(L_j - \frac{\varepsilon_n}{\Omega} T_1 + T_2)\ \Phi_j(s) = 0 \qquad (2)$$

where

$$L_j = b_\theta(\hat{s}^2 d^2/ds^2 - 1) - \frac{\tau(\Omega-1)}{\Omega\tau+1+\eta_i} + \frac{\Omega\tau+1+\eta_i(1-2b_\theta/\tau)}{\Omega\tau+1+\eta_i}\ \frac{(s-j)^2}{\Omega^2\eta_s^2}, \qquad (3)$$

$$T_1\ \Phi_j = \frac{\Omega\tau+1+\eta_i(1-5b_\theta/2\tau)}{\Omega\tau+1+\eta_i}[\Phi_{j+1}(s)+\Phi_{j-1}(s)+\hat{s}\ \frac{d}{ds}(\Phi_{j-1}(s)-\Phi_{j+1}(s))], \qquad (4)$$

$$T_2\ \Phi_j = H\int_0^1 \frac{d\kappa^2}{K(\kappa)}\sum_{p=-\infty}^{\infty} G(s-j,\kappa)\Phi_p(s)\ G(s-p,\kappa), \qquad (5)$$

$$H = \frac{(2\varepsilon/\pi)^{1/2}\Omega\tau}{\Omega\tau+1+\eta_i}\int_0^\infty \frac{dt\ \exp(-t^2)t^{1/2}[(\Omega-1)-\eta_e(t-3/2)]}{(\Omega-\varepsilon_n t+i\nu_{eff}t^{-3/2})}, \qquad (6)$$

$$G(s-p,\kappa) = \int_{-\theta_o}^{\theta_o} d\theta\ \exp(-i(s-p)\theta)/(\kappa^2-\sin^2\ \theta/2)^{1/2}, \qquad (7)$$

and $b_\theta = k_\theta^2\rho_s^2$, $\tau = T_e/T_i$, $\rho_s = C_s/\omega_{ci}$, $\varepsilon_n = r_n/R$, $r_n = |d\ell nN(r)/dr|$, $\eta_s = qb_\theta^{1/2}/\varepsilon_n$, $\nu_{eff} = \frac{\nu_{ei}}{\varepsilon\omega_{*e}}$, $\eta_{e,i} = (d\ell nT/d\ell nN)_{e,i}$. $K(\kappa)$ is the complete elliptic integral of the first kind with κ, the pitch angle, defined by $\kappa^2 = [\frac{1}{2}v^2-\mu B_o(1-\varepsilon)]/2\varepsilon\mu B_o$ and $\theta_o = 2\ \sin^{-1}(\kappa)$.
In Eq. (2), we have neglected the non-adiabatic circulating electron response and trapped-electron non-bounce averaged response.

We employ the large n ordering which leads to the ballooning-mode formalism. In the zeroth order, we have, with $z = s-j$,

$\Phi_j(s) = \hat{\phi}(z)$ and $\Phi_{j+p}(s) = \hat{\phi}(z-p)$; i.e., there is no phase shift between adjacent eigenmodes centered at each mode-rational surface. This corresponds to close-spaced turning points in the global radial direction. Fourier transforming Eq. (2) and with $\phi(\eta) = \frac{1}{2\pi}\int \hat{\phi}(z)\exp(i\eta z)dz$, we obtain a 1D integro-differential equation

$$\left[\frac{d^2}{d\eta^2} + Q(\eta)\right]\phi(\eta) - DH\int_0^1 \frac{d\kappa^2}{4K(\kappa)} \sum_{p=-\infty}^{\infty} g(\kappa,\eta-2\pi p)\int_{-\infty}^{\infty} d\eta' g(\kappa,\eta')\phi(2\pi p-\eta') = 0, \tag{8}$$

where

$$D = \frac{\Omega^2\eta_s^2\ (\Omega\tau+1+\eta_i)}{\Omega\tau+1+\eta_i(1-2b_\theta/\tau)}, \tag{9}$$

$$Q(\eta) = D\ \Big[\frac{\Omega-1}{\Omega+(1+\eta_i)/\tau} + b_\theta(1+\hat{s}^2\eta^2)$$
$$+ \frac{2\epsilon_n}{\Omega}\ \frac{\Omega\tau+1+\eta_i(1-5b_\theta/2\tau)}{\Omega\tau+1+\eta_i}(\cos\eta+\hat{s}\eta\ \sin\eta)\Big] \tag{10}$$

and

$$g(\kappa,\eta) = \int_{-\theta_0}^{\theta_0} \frac{d\theta\,\delta(\theta-\eta)}{(\kappa^2-\sin^2\theta/2)^{\frac{1}{2}}}\ . \tag{11}$$

Equation (8) is the lowest-order ballooning-mode equation describing trapped-electron modes along the magnetic field lines. It yields perturbations centered at the outside of the torus. The boundary condition imposed on Eq. (8) is that for large η, it corresponds to outgoing wave energy propagation. We also note that the above procedure of obtaining the lowest-order ballooning mode equation is equivalent to the usual ballooning-mode formalism.[3] In obtaining Eq. (8), the Poisson sum formula[13] $\sum_p \exp(i\eta p) = 2\pi\sum_p \delta(\eta-2\pi p)$ has been employed. It is also obvious that the trapped electron response vanishes for ϕ being odd with respect to $\eta=0$. Therefore, we will only consider even solution of ϕ.

We will solve Eq. (8) by using standard perturbation technique with the trapped-electron term treated as perturbation which will be justified by comparing with numerical solutions of Eq. (8). Typically, tokamaks have shear, $\hat{s} > \frac{1}{2}$, and the potential $-Q(\eta)$ for toroidicity-induced branch has local potential wells shown by the solid curve in Fig. 1. To proceed with analytical investigation, we approximate $-Q(\eta)$ by a double potential well shown by dotted line in Fig. 1 with

$$Q(\eta) \cong \begin{cases} Q(\eta_c) + Q''(\eta_o)(\eta-\eta_o)^2/2, & \eta \geq 0 \\ Q(\eta_o) + Q''(\eta_o)(\eta+\eta_o)^2/2, & \eta \leq 0 \end{cases} \tag{12}$$

where η_o is determined by $Q'(\pm\eta_o) = 0$. The zeroth order equation of Eq. (8) can be rewritten as

$$[d^2/dt^2 - (\lambda+t^2/4)]\phi_o(t) = 0, \tag{13}$$

for $|\eta|\geq 0$, where $t^2 = (-2Q''(\eta_o))^{\frac{1}{2}}(\eta-\eta_o)^2$ and $\lambda = -Q(\eta_o)/(-2Q''(\eta_o))^{\frac{1}{2}}$. The solution of Eq. (13) with decaying asymptotic behavior is given by the parabolic cylinder function $\phi_o = U(\lambda,t)$[14] where

$$U(\lambda,t) = \{\cos[(\frac{\lambda}{2}+\frac{1}{4})\pi]\ \Gamma(\frac{1}{4}-\frac{\lambda}{2})\ M(\frac{\lambda}{2}+\frac{1}{4},\frac{1}{2},\frac{t^2}{2})/2^{\lambda/2+1/4}$$

$$-\sin[(\frac{\lambda}{2}+\frac{1}{4})\pi]\ \Gamma(\frac{3}{4}-\frac{\lambda}{2})\ t\ M(\frac{\lambda}{2}+\frac{3}{4},\frac{3}{2},\frac{t^2}{2})/2^{\lambda/2-1/4}\}\ \frac{\exp(-t^2/4)}{\sqrt{\pi}}, \tag{14}$$

Γ is the gamma function and M is the confluent hypergeometric function. The boundary condition at $\eta=0$ for even solution is given by

$$\frac{\partial}{\partial\eta} U(\lambda_o, t(\eta=0)) = 0, \tag{15}$$

which provides the eigenvalue λ_o and the zeroth order eigen-frequency Ω_o. Including the trapped-electron contribution perturbatively, the dispersion relation is given by

$$\lambda = \lambda_o + \lambda_1 \tag{16}$$

where

$$\lambda_1 = \bar{D}H \int_0^1 \frac{d\kappa^2}{4K(\kappa)} \sum_p \left(\int_{-\infty}^{\infty} d\eta g(\kappa,\eta)\phi_o(2\pi p-\eta)\right)^2 \Big/ \int_{-\infty}^{\infty} \phi_o{}^2 dt, \tag{17}$$

and

$$\bar{D} = D/(-2Q''(\eta_o))^{\frac{1}{4}}. \tag{18}$$

Note that λ_1 is evaluated at $\Omega=\Omega_o$. Equations (15) and (16) can be combined to give the eige...alue Ω when η_o is determined by $Q'(\eta_o) = 0$. Now,

$$Q'(\eta_o) = 2D\{b_\theta \hat{s}^2 \eta_o + \frac{\epsilon_n}{\Omega}[1 - 5\eta_i b_\theta/2\tau(\Omega\tau+1+\eta_i)]$$

$$((\hat{s}-1)\sin\eta_o + \hat{s}\,\eta_o \cos\eta_o)\} \tag{19}$$

since toroidicity-induced branch generally exists for $\frac{\epsilon_n}{\Omega} > b_\theta \hat{s}^2$ and $|\eta_o| > 1$, we find that $\eta_o \simeq \pi/2$ for $\hat{s} \sim 1$. Then, we have

$$Q''(\eta_o) \cong 2D\{b_\theta \hat{s}^2 - \frac{\epsilon_n \hat{s}\pi}{2\Omega}[1 - 5\eta_i b_\theta/2\tau(\Omega\tau+1+\eta_i)]\} \tag{20}$$

Thus, with $\eta_i b_\theta/[\tau(\Omega\tau+1+\eta_i)] << 1$ and $(-Q''(\eta_o))^{\frac{1}{2}} << |Q(\eta_o)|$ which is equivalent to the approximation of $-Q$ by two completely separated wells, the solution of Eq. (16) is approximately given by $\Omega = \Omega_o + \Omega_1$, $|\Omega_1| << |\Omega_o|$, where

$$\Omega_o \simeq \frac{1 - \hat{s}\epsilon_n\pi - (1+\eta_i)b_\theta(1+\hat{s}^2\pi^2/4)/\tau}{1+b_\theta(1+\hat{s}^2\pi^2/4)}, \tag{21}$$

and

$$\Omega_1 \simeq \frac{2[\frac{\epsilon_n \hat{s}\pi}{2\Omega_o}(1 - \frac{5}{2} b_\theta \eta_i/(\Omega+(1+\eta_i)/\tau)) - b_\theta \hat{s}^2]^{\frac{1}{2}} \lambda_1}{\eta_s[1+b_\theta(1+\hat{s}^2\pi^2/4)][(\Omega\tau+1+\eta_i)/(\Omega\tau+1+\eta_i(1-2b_\theta/\tau))]^{\frac{1}{2}}}. \tag{22}$$

It is important to point out that as τ decreases, $-Q_r(\eta=0)$ also decreases and becomes negative. Hence, the double-well structure reduces to a single-well structure with a small bump at the origin. The approximation of $Q(\eta)$ by Eq. (12) is still good and so are the dispersion relations, Eqs. (15) and (16). However, the approximation of $-Q''(\eta_o)$ by Eq. (20), which leads to the eigenfrequencies in Eqs. (21) and (22), breaks down.

From Eq. (17), we note that λ_1 is proportional to the trapped-electron energy integral H. Examining Eq. (6) we find that, for $t_0 \equiv (\frac{\nu_{ei}}{\varepsilon\Omega_o})^{2/3} < 1 < \frac{\Omega_o}{\varepsilon_n}$,

$$H \simeq \frac{(2\varepsilon/\pi)^{\frac{1}{2}}\Omega_o\tau}{\Omega_o\tau+1+\eta_i} \{[\frac{\eta_e}{2}(1+2\zeta^2+2\zeta^3 Z(\zeta))-(\Omega-1+\frac{3}{2}\eta_e)(1+\zeta Z(\zeta))]$$

$$\frac{\Omega_o}{\varepsilon_n}(\pi)^{\frac{1}{2}} - (\Omega_o-1+\frac{3}{2}\eta_e)(\frac{2+3i}{9})t_o{}^{3/2}\}, \qquad (23)$$

where $\zeta^2 = (\Omega_o/\varepsilon_n)[1+i(t_o\varepsilon_n/\Omega_o)^{3/2}]$, and Z is the plasma dispersion function. While for $t_o > \Omega_o/\varepsilon_n > 1$, we have $H \propto \nu_{ei}{}^{-1}$.

Numerical solution of the integro-differential Eq. (8) has been performed by using the cubic B-spline finite element method[12] in order to verify the perturbative treatment and provide more understanding. The values taken for the fixed parameters were $b_\theta = \varepsilon_n = 0.1$, $\eta_e = 1$, $\eta_i = 0$, $\tau = 10$, $\hat{s} = q = 1$. In Fig. 2, we show $\Omega(=\Omega_r+i\Omega_i)$ versus ν_{ei}/ω_{*e} for $\varepsilon = 0.1$. Perturbative solutions given by Eqs. (15) and (16) are also calculated numerically and shown in Fig. 2. We note that the agreement between perturbation theory and numerical solutions of Eq. (8) is very good. The behavior of Ω is consistent with that of H. Figure 3 shows Ω as a function of ε for $\nu_{ei}/\omega_{*e} = 0.1$. As ε gets larger, the results of the perturbative theory becomes worse but the behavior of Ω is still good. This implies that the trapped-electron response can be considered as perturbation (for modest value of ε)

and the dominant toroidal coupling effect is due to ion magnetic drifts. In the above numerical examples, we found that keeping only $p=0$ term in the trapped-electron response in Eq. (8) is sufficient because the mode structures are well localized within the interval $[-\pi,\pi]$. It must be emphasized that the analytical calculation presented in the present work is for $\hat{s} > \frac{1}{2}$ and deals with the toroidicity-induced eigenmode with wave energy trapped in the off-center wells of $-Q(\eta)$ which gives rise to instability.[7,14,15] The employment of the strong coupling approximations[6] which is equivalent to expanding $Q(\eta)$ around the origin will certainly lead to erroneous results.

Acknowledgment

This work was supported by the United States Department of Energy, Contract No. EY-76-C-02-3073.

REFERENCES

1. W. M. Tang, Nucl. Fusion 18, 1089 (1978).
2. E. A. Frieman, G. Rewoldt and W. M. Tang, PPPL-1560 (1979).
3. J. W. Connor, R. J. Hastie and J. B. Taylor, Phys. Rev. Lett. 40, 396 (1978); A. H. Glasser, In Proc. Finite Beta Theory Workshop, Varenna, 1977, ed. B. Coppi and W. Sadowski.
4. G. Rewoldt, W. M. Tang and E. A. Frieman, Phys. Fluids 20, 402 (1977).
5. L. D. Pearlstein and H. L. Berk, Phys. Rev. Lett. 23, 220 (1969).
6. J. B. Taylor, in Proc. of 6th Int. Conf. on Plasma Physics and Controlled Nuclear Fusion Research, Vol. 2 (IAEA, Vienna, 1977), p. 322.
7. L. Chen and C. Z. Cheng, PPPL-1562 (1979); see also R. J. Hastie, K. W. Hesketh and J. B. Taylor, Nucl. Fusion 19, 1223 (1979).
8. C. Z. Cheng and L. Chen, PPPL-1579 (1979).
9. L. Chen, M. S. Chance and C. Z. Cheng, PPPL-1570 (1979).
10. K. T. Tsang and P. J. Catto, Phys. Rev. Lett. 39, 1664 (1977).
11. S. Inoue, K. Itoh and S. K. Wong, Hiroshima University Report HIFT-13 (1979).
12. W. H. Miner, Jr., Ph.D. Thesis, University of Texas at Austin, 1978.
13. P. M. Morse and H. Feshback, "Methods of Theoretical Physics", (1953) p. 467.
14. Handbook of Mathematical Functions, ed. by M. Abramowitz and I. A. Stegun, National Bureau of Standards, AMS55.

15. J. C. Adam, G. Laval, R. Pellat, Nucl. Fusion 13, 47 (1973).

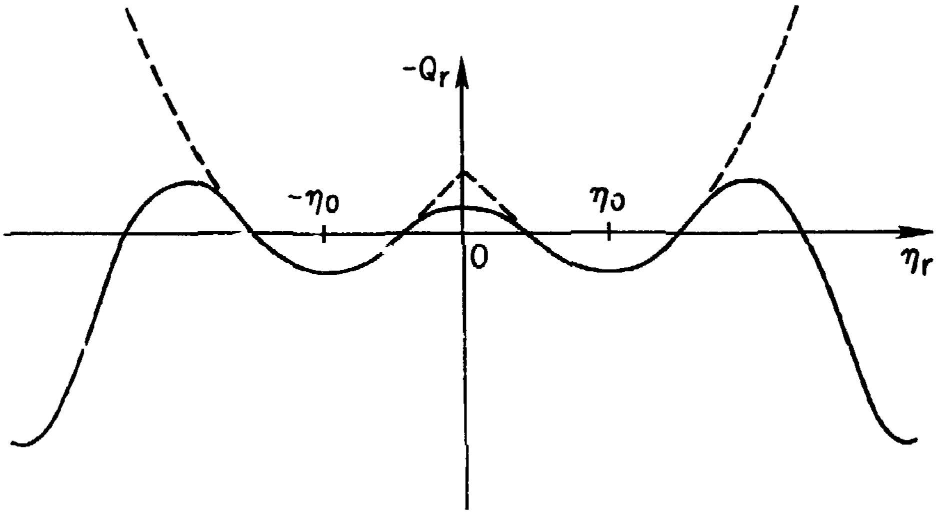

792621

Fig. 1. Typical potential structure of $-Q(\eta)$ for toroidicity-induced eigenmode branch with $\hat{s} > \frac{1}{2}$. The approximation of $-Q(\eta)$ is shown by the broken line.

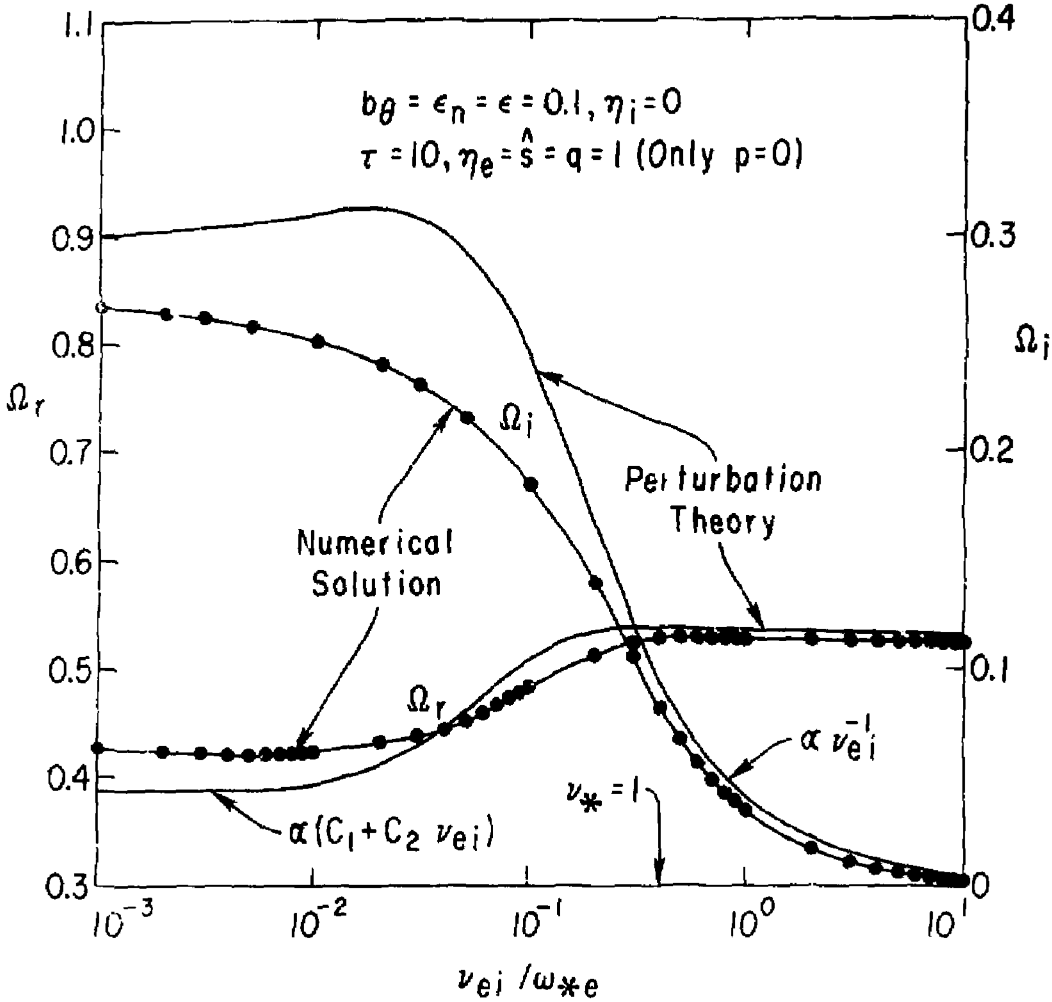

792622

Fig. 2. Plot of eigenmode frequencies Ω versus ν_{ei}/ω_{*e} for $b_\theta = \varepsilon = \varepsilon_n = 0.1$, $\tau = 10$, $\eta_i = 0$. Numerical solutions of Eq. (8) are compared with the results obtained from perturbation theory.

$\nu_* \equiv \nu_{ei}/(\varepsilon\omega_{be}) = (\nu_{ei}/\omega_{*e})(q/\varepsilon_n\varepsilon)(b_\theta m_e/\varepsilon m_i)^{\frac{1}{2}}$.

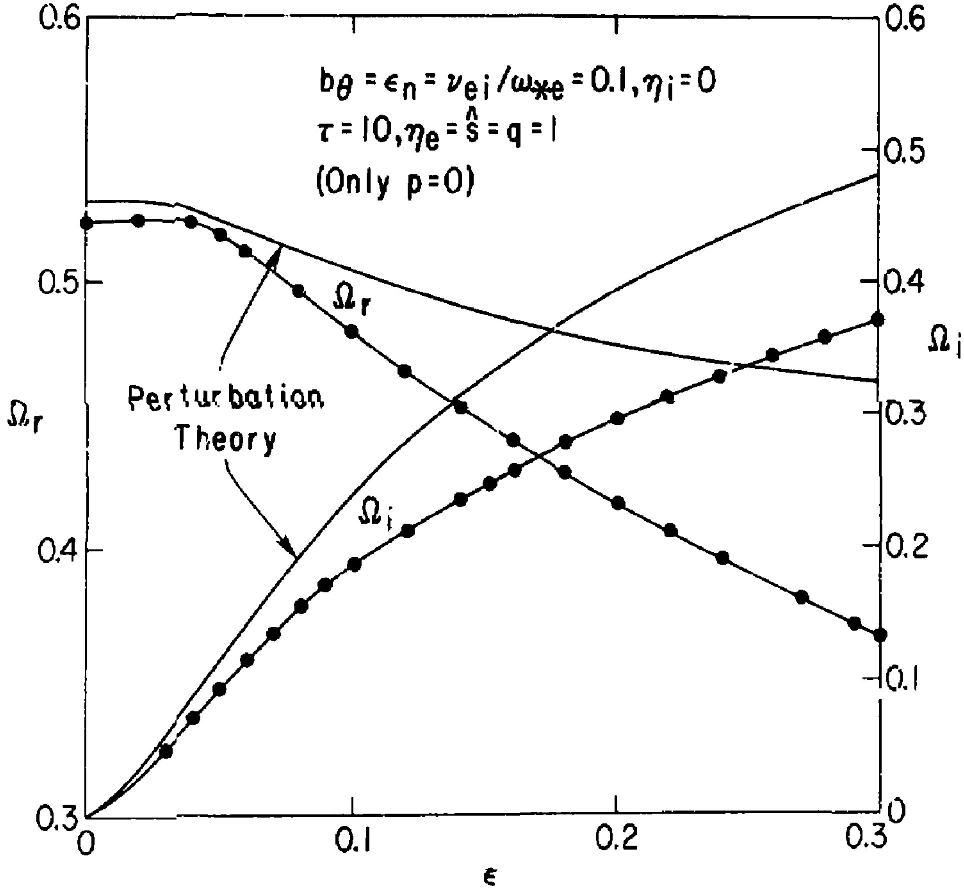

792623

Fig. 3. Plot of eigenmode frequencies Ω versus ϵ for $\nu_{ei}/\omega_{*e} = 0.1$. The other parameters are the same as in Fig. 2.